

Search for dark Higgs inflaton with curvature couplings at LHC experiments

Lucia Aurelia Popa

Institute of Space Science,
Bucharest-Magurele, Ro-077125 Romania

E-mail: lpopa@spacescience.ro

Abstract. We analyse the dark Higgs inflation model with curvature corrections and explore the possibility to test its predictions by the particle physics experiments at LHC.

We show that the dark Higgs inflation model with curvature corrections is strongly favoured by the present cosmological observation. The cosmological predictions of this model, including the quantum corrections of dark Higgs coupling constants and the uncertainty in estimation of the reheating temperature, lead to the dark Higgs mass $m_\phi = 0.919 \pm 0.211$ GeV and the mixing angle $\theta = 1.492 \pm 0.045$ (at 68% CL).

We evaluate the FASER and MAPP-1 experiments reach for dark Higgs inflaton mass and mixing angle in the 95% CL cosmological confidence region for an integrated luminosity of 3ab^{-1} at 13 TeV LHC, assuming 100% detection efficiency.

We conclude that the dark Higgs inflation model with curvature corrections is a compelling inflation scenario based on particle physics theory favoured by the present cosmological measurements that leaves imprints in the dark Higgs boson searches at LHC.

Keywords: cosmic microwave background, inflation, dark Higgs, cosmological observations, LHC experiments

Contents

1	Introduction	1
2	Dark Higgs inflaton properties	4
2.1	Dark Higgs inflaton parameters	4
2.2	Reheating and horizon crossing	6
3	Dark Higgs inflation with curvature corrections	6
4	Cosmological constraints	8
4.1	Parameterisation and methods	8
4.2	Analysis	10
5	Dark Higgs inflaton at LHC experiments	12
5.1	Dark Higgs inflaton decay inside detector	12
5.2	Dark Higgs inflaton production at LHC	14
5.3	LHC experiments reach for dark Higgs inflaton	15
6	Conclusion	15

1 Introduction

The precise Cosmic Microwave Background (CMB) properties reported by the PLANCK experiment [1–3] and the discovery by LHC of the Higgs boson [4, 5] increased the interest in so called Higgs portal interactions that connect the hidden (dark) sector and the visible sector of the Standard Model (SM), with expected imprints on collider experiments [6]. Scenarios beyond-the-SM (BSM), that introduce a dark sector in addition to the visible SM sector are required to explain a number of observed phenomena in particle physics, astrophysics and cosmology such as the non-zero neutrino masses and oscillations, the Dark Matter (DM), baryon asymmetry of the universe, the cosmological inflation.

It is usual to assume that cosmic inflation is decoupled from the SM at energies lower than the inflationary scale since the slow-roll conditions for inflation generally permit only tiny couplings of the inflaton field to other fields. This assumption prevents the direct investigation of inflation mechanism in particle physics experiments. Consequently, there are little compelling scenarios of inflation based on particle physics theory.

Since the only known fundamental scalar quantum field is the SM Higgs field, the inflation models using the SM Higgs boson as inflaton attained great attention over the past years. A number of Higgs inflation models, mostly with non-canonical action, have been

proposed. They include models with Higgs scalar field non-minimally coupled to gravity [7–9], non-minimal derivative coupling to the Einstein tensor [10–13], scalar-tensor models [14, 15], Galileon models [16–19], quartic hilltop models [24, 25].

The viability of these models is already substantially limited mostly because they predict tensor-to-scalar ratios larger than the upper bound set by the combined analysis of PLANCK and BICEP-Keck Array data (hereafter PLANCK+BK15) that constrain the energy scale of inflation to [2, 3]:

$$V_*^{1/4} = \left(\frac{3\pi^2 A_s^*}{2} r_* \right)^{1/4} M_{pl} < 1.6 \times 10^{16} \text{GeV} \quad (95\% \text{CL}). \quad (1.1)$$

Here the quantities with (*) are evaluated at the pivot scale $k_* = 0.002$, r_* is the ratio of tensor-to-scalar amplitudes, A_s^* is the amplitude of the curvature density perturbations and M_{pl} is the reduced Planck mass. This imply an upper bound for the Hubble expansion rate during inflation:

$$H_* < 2.5 \times 10^{-5} M_{pl} \quad (95\% \text{CL}). \quad (1.2)$$

The above bound selects the viable Higgs inflation models from the requirement $H_* \ll \Lambda_c$, where Λ_c is the unitary bound of each underlying theory, defined as the scale below which the quantum gravitational corrections are sub-leading [20–22].

It worths to mention that the chaotic inflation model with quartic potential is excluded by the data at more than 95% confidence level [23].

Among the models used to lower the predictions for tensor-to-scalar ratio, the most studied is the Higgs inflation with non-minimal coupling to gravity [7]. At tree level and for large non-minimal coupling $\xi \sim \mathcal{O}(10^4)$, this model gives a small tensor-to-scalar ratio, in agreement with the PLANCK+BK15 data. However, for such large values of ξ the unitary bound scale, $\Lambda_c = M_{pl}/\xi$, could be close or below the energy scale of inflation [20, 26].

An interesting framework for Higgs inflation is provided the scalar-tensor models including the non-minimal kinetic coupling to the Einstein tensor and to the Gauss-Bonnet invariant. These models can produce inflation simultaneously satisfying the present inflationary observational constrains and the unitary bound constraints [14, 15].

Higgs portal interactions via the Renormalisation Group (RG) loop contributions can also lower the predictions of Higgs inflation models for the tensor-to-scalar ratio. The price to pay in these models is the electroweak (EW) vacuum metastability issue. The actual values of Higgs boson and top quark masses imply that the EW vacuum is metastable at energies larger than $\Lambda_I \sim 10^{11}$ GeV, where Higgs quartic coupling turns negative¹[27–30].

However, it is found that a small admixture of the Higgs field with a SM scalar singlet with non-zero vacuum expectation value (vev) can make the EW completely stable due to a tree-level effect on the Higgs quartic coupling which may be enough to guarantees the stability at large Higgs field values [32–34].

An appealing scenario in the presence of Higgs portal interactions is given by a SM singlet scalar field with non-zero vev mixed with the SM Higgs boson, often called dark Higgs boson. The dark Higgs mixing with the SM Higgs boson make possible the direct search of the dark Higgs inflaton at collider experiments. The mixing guarantee that dark Higgs can

¹The actual value of EW vacuum metastability scale is defined for the top quark mass $m_t = 173.15$ GeV and Higgs boson mass $m_H = 125.10$ GeV [31] as the value of the Higgs field at which the Higgs quartic coupling, λ_h , becomes negative due to radiative corrections.

be produced in the same channels as the SM Higgs boson if its mass would be the same as that of the dark Higgs boson. Through the same mixing the dark Higgs boson inherits the SM Higgs boson couplings to SM fermions via the Yukawa interaction term:

$$L \supset \theta \frac{m_f}{v} \phi \bar{f} f, \quad (1.3)$$

where: ϕ is the dark Higgs field, θ is its mixing angle with SM Higgs boson and m_f is the fermion mass.

Dark Higgs bosons can be produced at LHC in rare heavy meson decays (such as K and B mesons). They are highly collimated, with characteristic angles $\alpha = M/E$ relative to the parent meson's direction (M is the meson mass and E is the dark Higgs energy). For $E \sim 1$ TeV the light dark Higgs decay lengths are of $\mathcal{O}(10^3 m)$. Therefore a significant number of dark Higgs bosons can be detected in faraway detectors of the LHC experiments [6]. Thus, present and future experimental sensitivity to the light dark Higgs boson decay crucially depends on its production and decay rates and on detector's location and acceptance.

The light dark Higgs boson as inflaton (rather than the Higgs boson) has been first implemented in Ref. [37], extending the ν MSM model [38, 39] to simultaneously explain the cosmological inflation, the DM sterile neutrino masses and the baryon asymmetry of the universe [37, 40]. The light dark Higgs inflaton properties has been mostly studied in the frame of dark Higgs inflation with non-minimal coupling to gravity [41, 42, 44, 53]. Refs.[45, 46] present a detailed analysis on the possibility to explore this model in the particle physics experiments.

This possibility has been also investigated in the frame of low-scale inflation models, such the quartic hilltop model [24] that predicting a very small value for tensor-to scalar ratio, beyond the sensitivity of the CMB experiments. Thus, the dark Higgs searchers at LHC could experimentally test the low-scale of inflation.

In this paper we analyse the dark Higgs inflation model with curvature corrections given by the kinetic term non-minimally coupled to the Einstein tensor and the coupling to the Gauss-Bonnet (GB) 4-dimensional invariant (hereafter EGB dark Higgs inflation) and explore the possibility to test its predictions by the particle physics experiments.

In this model, the non-minimal kinetic coupling to the Einstein tensor causes the inflaton field to roll slower, avoiding the problem of large fields present in chaotic inflation [11]. On the other hand, the second-order curvature corrections represented by the scalar field coupled to the GB term can increment or suppress (depending on the sign) the tensor-to-scalar ratio [47–49]. The dynamics of the slow-roll inflation by combining both corrections has been proposed in context of the SM Higgs inflation in Refs.[14, 15].

The possibility to explore this model by the dark Higgs searchers at LHC could provide connections between fundamental theories like supergravity and string theories where these couplings are expected to arise, and the Higgs portal interactions.

The paper is organised as follows. In the next section we discuss the dark Higgs inflaton properties. In Section 3 we introduce the EGB dark Higgs inflation model. In Section 4 we analyse the cosmological consistency of the EGB dark Higgs inflation predictions. Section 5 discuss the possibility to test the EGB dark Higgs inflation predictions by some representative particle physics experiments at LHC. In Section 6 we draw our conclusions.

Throughout the paper we consider an homogeneous and isotropic flat background described

by the Friedmann-Robertson-Walker (FRW) metric:

$$ds^2 = g_{\mu,\nu}dx_\mu dx^\nu = -dt^2 + a^2(t)dx^2, \quad (1.4)$$

where a is the cosmological scale factor ($a_0=1$ today). Also, we use the overdot to denote the time derivative and $(')$ to denote the derivative with respect to the scalar field.

2 Dark Higgs inflaton properties

2.1 Dark Higgs inflaton parameters

We consider the extension of the SM canonical action with the dark Higgs inflaton field, as introduced in Ref. [37]:

$$S = \int d^4x \sqrt{-g} \left[\frac{\mathcal{R}}{2\kappa^2} + \frac{1}{2}(\partial_\mu\phi)^2 - V(\phi) \right], \quad (2.1)$$

where \mathcal{R} is the Ricci scalar, $\kappa^2 = M_{pl}^{-2}$, ϕ is the dark Higgs inflaton field with the potential $V(\phi)$ defined as:

$$V(\phi) = -\frac{1}{2}m_\phi^2\phi^2 + \frac{\beta}{4}\phi^4 + \lambda \left(\mathcal{H}^\dagger\mathcal{H} - \frac{\alpha}{\lambda}\phi^2 \right)^2. \quad (2.2)$$

In the above equation λ is the SM Higgs field self coupling, m_ϕ is the dark Higgs mass, β is the dark Higgs quartic coupling and α is the coupling between the SM Higgs field \mathcal{H} and the dark Higgs inflaton. For $\alpha, \beta \ll \lambda$, inflation is driven along a flat direction of the scalar potential given by:

$$\mathcal{H}^\dagger\mathcal{H} \simeq \frac{\alpha}{\lambda}\phi^2. \quad (2.3)$$

Along this direction the dark Higgs potential is $V(\phi) = \beta\phi^4/4$ and the coupling constant β can be fixed from the requirement to obtain the correct the amplitude of the curvature density perturbations. This condition leads to $\beta \sim 1.3 \times 10^{-13}$ [50].

The negative sign of the quadratic term in (2.2) ensures that the scale invariance is explicitly broken on the classical level in the inflaton sector, leading to non-zero vev for the dark Higgs inflaton after reheating. Then, the condition (2.3) gives rise to EW spontaneous symmetry breaking and the SM Higgs field gains non-zero vev too.

We remind that the SM Higgs boson mass is given by $m_H = \sqrt{2\lambda}v$, where the SM Higgs vev is fixed at $v \equiv (\sqrt{2}G_F)^{1/2} = 246.22$ GeV by the Fermi coupling constant G_F , and the experimentally measured Higgs boson mass is $m_H = 125.10 \pm 0.14$ GeV [31].

In the gauge base $(\sqrt{2}\mathcal{H} - v, \phi)$ the dark Higgs field expectation value, $\langle \phi \rangle$, its mass m_ϕ and mixing angle θ , are given by:

$$\langle \phi \rangle = \frac{m_H}{2\sqrt{\alpha}}, \quad m_\phi = m_H \sqrt{\frac{\beta}{2\alpha}}, \quad \theta = \sqrt{\frac{2\alpha}{\lambda}}. \quad (2.4)$$

For the purpose of this work we choose $\alpha > \beta/2$, therefore the dark Higgs inflaton is lighter than the SM Higgs boson, $m_\phi < m_H$.

The upper bound on the coupling constant α comes from the requirement that the quantum corrections do not upset the flatness of the inflation potential. This constrain leads

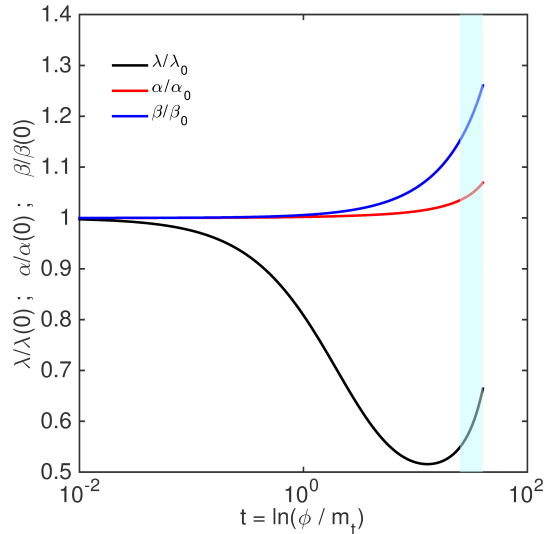


Figure 1. The evolution with the scale dependent variable $t = \ln(\phi/m_t)$ of the running of λ , β and α coupling constants normalised to their initial values chosen at $t = 0$ as: $\lambda(0) = 0.129$, $\beta(0) = 1.3 \times 10^{-13}$ and $\alpha(0) = 3 \times 10^{-7}$. The SM Higgs mass is fixed at $m_H = 125.09$ GeV. The right-hand blue region indicates the slow-roll inflationary regime.

to $\alpha < 3 \times 10^{-7}$ at the tree level [45] and corresponds to the lower bound of the dark Higgs inflaton mass:

$$m_\phi \geq 0.058 \left(\frac{\beta}{1.3 \times 10^{-13}} \right)^{1/2} \text{ GeV}. \quad (2.5)$$

The lower bound on α comes from the requirement to have an efficient conversion of the lepton asymmetry to baryon asymmetry during baryogenesis. This requirement leads to $\alpha > \beta \sim 10^{-13}$ [37]. A stronger lower bound on α is placed by the estimate of the reheating temperature. For the inflaton particles in thermal equilibrium the reheating temperature is given by [40]:

$$T_r \simeq \frac{\zeta(3)\alpha^2}{4\pi^2} \sqrt{\frac{90}{g_r}} M_{\text{pl}}, \quad (2.6)$$

where $g_r = 106.75$ is the SM effective number of relativistic degrees of freedom at reheating and $\zeta(3) = 1.202$ is the Reimann zeta function. The requirement that $T_r > 150$ GeV ($T \simeq 150$ GeV is the temperature of the EW symmetry breaking), leads to $\alpha > 7.3 \times 10^{-8}$.

For a non-thermal distribution of the inflaton field the estimate of the reheating temperature is $\sim 10^5 T_r$ [51, 52], leading to $\alpha > 7 \times 10^{-10}$.

These constraints are consistent to the upper bounds of the dark Higgs inflaton mass [40]:

$$m_\phi \leq (0.116 - 1.166) \left(\frac{\beta}{1.3 \times 10^{-13}} \right)^{1/2} \text{ GeV}, \quad (2.7)$$

where the range corresponds to the thermal or non-thermal estimates.

The above bounds of the inflaton mass may be changed if the quantum corrections of the coupling constants are taken into account.

Figure 1 presents the evolution with the scale dependent variable $t = \ln(\phi/m_t)$ of the running

of $\lambda(t)$, $\beta(t)$ and $\alpha(t)$ coupling constants normalised to their initial values $\lambda(0)$, $\beta(0)$ and $\alpha(0)$, obtained by the integration the corresponding beta functions [29, 41, 44, 53].

As the SM Higgs mass is fixed at $m_H = 125.09$ GeV we take $\lambda(0) = 0.129$. We also fix $\alpha(0) = 3 \times 10^{-7}$ to the α upper bound and take $\beta(0) = 1.3 \times 10^{-13}$.

One should note that the correction to β from the coupling of the dark Higgs inflaton to the SM Higgs boson is $\delta\beta \sim \alpha^2$ and therefore the evolution of β is dominated by the α^2 contribution. Figure 1 shows that all coupling constants remain positive at the inflationary scale while the flatness of the inflationary potential is preserved.

2.2 Reheating and horizon crossing

The reheating proceeds by the energy transfer from the dark Higgs inflaton field to the SM Higgs particles through a regime of parametric resonance [51, 52]. At early stages the entire energy is in the inflaton zero-mode and all other modes are absent. The inflaton zero-mode oscillations excite the non-zero modes of the inflaton and of the SM Higgs particles. This parametric resonance regime ends before a significant part of the inflaton zero-mode energy is depleted [40]. The reason is the SM Higgs re-scattering process that become important quite early because of the large SM Higgs self-coupling ($\lambda \sim 0.1$).

After the end of the parametric resonance regime, the fluctuations of the inflaton field continue to grow exponentially while the energy transferred to the SM Higgs field is negligible small. The SM Higgs re-scattering processes bring the inflaton particles in the thermal equilibrium and the reheating proceeds through the decay of the dark Higgs inflaton into the SM Higgs particles.

The inflationary observables are evaluated at the epoch of the Hubble crossing scale k_* (pivot scale) quantified by the number of e -folds \mathcal{N} before the end of the inflation. Therefore, the uncertainties in the determination of \mathcal{N} translates into theoretical uncertainties in determination of the inflationary observables [41, 54]. Assuming that the ratio of the today entropy per co-moving volume to that after reheating is negligible, the main error $\Delta\mathcal{N}$ in the determination of \mathcal{N} is given by the uncertainty in the determination of the reheating temperature T_r . The number of e -foldings at Hubble crossing scale k_* is related to T_r through:

$$\mathcal{N} = \log \left[\left(\frac{\rho_r}{\rho_e} \right)^{1/4} \left(\frac{g_0 T_0^3}{g_r T_r^3} \right)^{1/3} \left(\frac{k_*}{a_0 H_0} \right) \right], \quad (2.8)$$

where ρ_r and ρ_e refer to the densities at reheating and at end of inflation, T_0 is the present photon temperature, H_* is the Hubble parameter at k_* , $g_r = 106.75$ and $g_0 = 43/11$ are the effective number of relativistic degrees of freedom at reheating and at present time.

From (2.6) and (2.8) we get $\Delta\mathcal{N} \simeq 3$ corresponding to the uncertainty in determination of T_r for to a thermal distribution of the inflaton. This uncertainty is four times higher, $\Delta\mathcal{N} \simeq 12$, in the case of non-thermal distribution.

3 Dark Higgs inflation with curvature corrections

Closely following [14, 15], in this section we introduce the inflation model assuming non-minimal coupling of the dark Higgs field with the Einstein tensor and to the Gauss-Bonnet (GB) 4 - dimensional invariant (the EGB dark Higgs inflation model), derive the background

field equations, the slow-roll parameters and evaluate the primordial power spectra the the scalar and tensor perturbations.

The action of this model is:

$$S_E = \int d^4x \sqrt{-g} \left[\frac{\mathcal{R}}{2\kappa^2} + X - V(\phi) + F_1(\phi)G_{\mu\nu}\partial^\mu\phi\partial^\nu\phi - F_2(\phi)\mathcal{G} \right], \quad (3.1)$$

where $V(\phi)$ is the dark Higgs potential given in (2.2), $F_1(\phi)$ and $F_2(\phi)$ are coupling functions, $G_{\mu\nu}$ is the Einstein tensor, \mathcal{G} is the GB 4-dimensional invariant:

$$\mathcal{G} = \mathcal{R}^2 - 4\mathcal{R}_{\mu\nu}\mathcal{R}^{\mu\nu} + \mathcal{R}_{\mu\nu\delta\rho}\mathcal{R}^{\mu\nu\delta\rho}. \quad (3.2)$$

The field equations in a spatially flat background described by the FRW metric (1.4) are of the form (see Appendix B from [15]) :

$$H^2 = \frac{\kappa^2}{3} \left(\frac{1}{2} + V(\phi) + 9H^2F_1\dot{\phi}^2 + 24H^3\dot{F}_2 \right), \quad (3.3)$$

$$\begin{aligned} \ddot{\phi} + 3H\dot{\phi} + V' + 24H^2(H^2 + \dot{H})F_2' + 18H^3F_1\dot{\phi} \\ + 12H\dot{H}F_1\dot{\phi} + 6 * H^2F_1\ddot{\phi} + 3H^2F_1' + \dot{\phi}^2 = 0. \end{aligned} \quad (3.4)$$

The slow-roll parameters are defined as:

$$\epsilon_0 = -\frac{\dot{H}}{H^2}, \quad \epsilon_1 = \frac{\dot{\epsilon}_0}{H\epsilon_0}, \quad k_0 = 3F_1\dot{\phi}^2, \quad k_1 = \frac{\dot{k}_0}{Hk_0}, \quad \Delta_0 = 8H\dot{F}_2, \quad \Delta_1 = \frac{\dot{\Delta}_0}{H\Delta_0}. \quad (3.5)$$

Under the slow-roll conditions $\ddot{\phi} \ll 3H\dot{\phi}$ and $|\epsilon_0|, |\epsilon_1|, \dots, |\Delta_1| \ll 1$ the potential and field equations take the form:

$$H^2 \simeq \frac{\kappa^2}{3}V(\phi) \quad (3.6)$$

$$3H\dot{\phi} \simeq -V' - 18H^3F_1\dot{\phi} - 24H^4F_2'. \quad (3.7)$$

The number of e -folds before the end of inflation expressed in terms of the inflaton field is given by:

$$\mathcal{N} = \int_{\phi_I}^{\phi_E} \frac{H}{\dot{\phi}} d\phi = \int_{\phi_{\mathcal{N}}}^{\phi_e} \frac{H^2 + 6H^4F_1}{-8H^4F_2' - \frac{1}{3}V'} d\phi, \quad (3.8)$$

where ϕ_I and ϕ_E are the values of the inflaton field at the begging and at the end of inflation. The power spectra of the primordial scalar and tensor perturbations, $\mathcal{P}_{\mathcal{R}}$ and $\mathcal{P}_{\mathcal{T}}$, are computed as:

$$\begin{aligned} \mathcal{P}_{\mathcal{R}} = A_S \frac{H^2}{2\pi^2} \frac{\mathcal{G}_S^{1/2}}{\mathcal{F}_S^{3/2}}, \quad A_S = \frac{1}{2} 2^{2\mu_S-3} \left| \frac{\Gamma(\mu_S)}{\Gamma(3/2)} \right|^2, \quad \mu_S^2 = \frac{9}{4} \left[1 + \frac{4}{3}\epsilon_0 + \frac{2}{3} \frac{2\epsilon_0\epsilon_1 - \Delta_0\Delta_1}{2\epsilon_0 - \Delta_0} \right] \\ \mathcal{P}_{\mathcal{T}} = 16A_T \frac{H^2}{2\pi^2} \frac{\mathcal{G}_T^{1/2}}{\mathcal{F}_T^{3/2}}, \quad A_T = \frac{1}{2} 2^{2\mu_T-3} \left| \frac{\Gamma(\mu_T)}{\Gamma(3/2)} \right|^2, \quad \mu_T = \frac{3}{2} + \epsilon_0, \end{aligned} \quad (3.9)$$

$$\begin{aligned} \mathcal{F}_S = c_S^2 \mathcal{G}_S, \quad \mathcal{G}_S = \epsilon_0 - \frac{1}{2}\Delta_0, \quad c_S^2 = 1 - \frac{\frac{4}{3}k_0(\Delta_0 + \frac{4}{3}k_0) + \frac{4}{3}k_0\epsilon_0}{2\epsilon_0 - \Delta_0}, \\ \mathcal{F}_T = c_T^2 \mathcal{G}_T, \quad \mathcal{G}_T = 1 - \frac{1}{3}k_0 - \Delta_0, \quad c_T^2 = \frac{3 + k_0 - 3\Delta_0(\epsilon_0 + \Delta_1)}{3 - k_0 - 3\Delta_0}, \end{aligned} \quad (3.10)$$

where c_S and c_T are the sound speeds of scalar and tensor density perturbations. The spectral index of scalar density perturbations n_S and the tensor-to-scalar ratio expressed in terms of slow-roll parameters are given by:

$$n_S = -2\epsilon_0 - \frac{2\epsilon_0\epsilon_1 - \Delta_0\Delta_1}{2\epsilon_0 - \Delta_0}. \quad (3.11)$$

$$r = 8 \left(\frac{2\epsilon_0 - \Delta_0}{1 - \frac{1}{3}k_0 - \Delta_0} \right). \quad (3.12)$$

Hereafter we take $F_1(\phi)$ and $F_2(\phi)$ power-law functions of the form:

$$F_1(\phi) = \frac{\gamma}{\phi^4}, \quad F_2(\phi) = \frac{\eta}{\phi^4}, \quad (3.13)$$

where γ and η are positive constants with the dimension $[\gamma] = M_{pl}^2$ and $[\eta] = M_{pl}^4$. For this setup, the first slow-roll parameter ϵ_0 reads as:

$$\epsilon_0 = \frac{16}{3} \frac{(3 - 2\eta\beta)}{(2 + \gamma\beta)\phi^2}. \quad (3.14)$$

From (3.8) one gets the number of e -folds before the end of inflation:

$$\mathcal{N} = - \left. \frac{3(2 + \gamma\beta)}{16(3 - 2\eta\beta)} \phi^2 \right|_{\phi_I}^{\phi_E}. \quad (3.15)$$

The value of the scalar field at the end of inflation, ϕ_E , is obtained from the requirement $\epsilon_0 = 1$, while (3.15) allows the determination of the inflaton field value ϕ_I at \mathcal{N} e -folds before the end of inflation:

$$\phi_E = \frac{4\sqrt{3 - 2\eta\beta}}{\sqrt{3(2 + \gamma\beta)}}, \quad \phi_I = \sqrt{\mathcal{N} + 1} \phi_E. \quad (3.16)$$

4 Cosmological constraints

4.1 Parameterisation and methods

The dark Higgs baseline cosmological model is described by the following parameters:

$$\mathbf{P} = \{ \Omega_b h^2, \Omega_c h^2, \theta_s, \tau, \log(10^{10} A_s), n_s, \mathcal{N}, \beta, \alpha \}, \quad (4.1)$$

where: $\Omega_b h^2$ is the present baryon energy density, $\Omega_c h^2$ is the present CDM energy density, θ_s is the ratio of sound horizon to angular diameter distance at decoupling, τ is the optical depth at reionization, A_s and n_s are the amplitude and the spectral index of the primordial curvature perturbations, \mathcal{N} is the number of e -folds introduced to account for the uncertainty in the determination of the reheating temperature, β is the dark Higgs quartic coupling and α is the dark Higgs - SM Higgs coupling constant.

The EGB dark Higgs inflation model extends the dark Higgs baseline model by including the following parameters:

$$\mathbf{P}_{\text{EGB}} = \{ \gamma\beta, \eta\beta \}, \quad (4.2)$$

where the coupling constants γ and β are defined in (3.13).

We compute the dependence on the scaling variable $t = \ln(\phi/m_t)$ of the running of various coupling constants by integrating the corresponding beta functions:

$$Y(t) = \int_0^t \beta_Y dt, \quad Y = \{g, g', g_s, y_t, \beta, \alpha\}, \quad (4.3)$$

where g, g', g_s are the gauge couplings, y_t is the Yukawa coupling, β is the dark Higgs quartic coupling and α is the dark Higgs - SM Higgs coupling (for the relevant beta functions see Appendix A from [44] and references therein).

At $t = 0$ the SM Higgs self coupling $\lambda(0) = 0.129$ and the top Yukawa coupling $y_t(0) = 0.976$ are fixed by the SM Higgs and top quark pole masses [29]. For the gauge couplings at $t = 0$ we take $g'(0) = 0.364$, $g(0) = 0.64$ and $g_s(0) = 1.161$ [55]. The priors for $\beta(0)$ and $\alpha(0)$ are given in Table 1 (see below).

We modify the standard Boltzmann code `camb`² [56] to calculate the primordial power spectra of scalar $\mathcal{P}_R(k)$ and tensor $\mathcal{P}_T(k)$ density perturbations for the dark Higgs inflation model with curvature corrections presented in the previous section. The code evolves the coupled dark Higgs field equations (3.3) and (3.4) with respect to the conformal time for wave numbers in the range $5 \times 10^6 - 5 \text{ Mpc}^{-1}$ and evaluate the RG corrections to the coupling constants as presented before. The value of the inflaton field ϕ_I and ϕ_E at the beginning and at the end of inflation are obtained from (3.16). The primordial power spectra $\mathcal{P}_R(k)$ and $\mathcal{P}_T(k)$ are obtained from (3.9) with the slow-roll parameters defined in (3.5).

The scalar spectral index of the curvature perturbations n_S and the ratio of tensor-to-scalar amplitudes r are then evaluated at the pivot scale $k_* = 0.002 \text{ Mpc}^{-1}$ as:

$$n_S = \left. \frac{d \ln \mathcal{P}_R(k)}{d \ln k} \right|_{k_*}, \quad r = \left. \frac{\mathcal{P}_T(k)}{\mathcal{P}_R(k)} \right|_{k_*}. \quad (4.4)$$

The extraction of parameters from the cosmological dataset is based on Monte-Carlo Markov Chains (MCMC) technique. We modify the publicly available version of the package `CosmoMC`³ [57] to sample from the space of dark Higgs inflation model parameters and generate estimates of their posterior mean and confidence intervals.

We made some test runs to optimise the parameters prior intervals and sampling. The final run is based on 120 independent chains, reaching the convergence criterion $(R - 1) \simeq 0.01$. The $(R - 1)$ criterion is defined as the ratio between the variance of the means and the mean of variances for the second half of chains [57].

We assume a flat universe and uniform priors for all parameters adopted in the analysis in the intervals listed in Table 1. The Hubble expansion rate H_0 is a derived parameter in our analysis. We constrained H_0 values to reject the extreme models.

For the cosmological analysis we use the CMB temperature (TT), polarization (EE, TE) and lensing angular power spectra from PLANCK 2018 release [1] and the likelihood codes corresponding to different multipole ranges [58]⁴. The PLANCK data currently provide the best characterisation of the primordial density perturbations [2], constraining the cosmological parameters at the sub-percent level [1].

²<http://camb.info>

³<http://cosmologist.info/cosmomc/>

⁴<http://pla.esac.esa.int/pla/cosmology>

Table 1. Priors and constraints on EGB dark Higgs inflation model parameters adopted in the analysis. All priors are uniform in the listed intervals. We assume a flat universe.

Parameter	Prior
$\Omega_b h^2$	[0.005, 0.1]
$\Omega_c h^2$	[0.001, 0.5]
$100\theta_s$	[0.5, 10]
τ	[0.01, 0.9]
$\log(10^{10} A_s)$	[2.5, 5]
n_s	[0.5, 1.5]
\mathcal{N}	[54, 64]
$\alpha \times 10^7$	[0.007, 3]
$\beta \times 10^{13}$	[1, 5]
$\gamma\beta$	[0, 3]
$\eta\beta$	[0, 3]
$H_0(\text{km s}^{-1}\text{Mpc}^{-1})$	[20, 100]

We use the following combinations of TT, TE, EE and lensing PLANCK likelihoods [2]: (i) Planck TT+lowE: the combination of high- l TT likelihood at multipoles $l \geq 30$, the Commander likelihood for low- l temperature-only and the SimAll low- l EE likelihood in the range $2 < l < 29$; (ii) PLANCK TE and Planck EE: the combination of TE and EE likelihoods at $l \geq 30$; (iii) PLANCK TT,TE,EE+lowE: the combination of Commander likelihood using TT, TE, and EE spectra at $l \geq 30$, the low- l temperature, and the low- SimAll EE likelihood; (iv) PLANCK TT,TE,EE+lowP: the combination of the likelihoods using TT, TE, and EE spectra at $l > 30$; (v) PLANCK high- l and Planck low- l polarization: the Plik likelihood; (vi) PLANCK CMB lensing: the CMB lensing likelihood [59] for lensing multipoles $8 < l < 400$.

We also consider the measurement of the CMB B-mode polarization angular power spectrum by the BICEP2/Keck Array collaboration [3]. The BK15 likelihood B-mode polarization only leads to an upper limit of tensor-to-scalar ratio amplitudes $r < 0.07$ (95% CL) [3].

We will refer to the combination of these datasets as PLANCK TT,TE,EE+lowE+lensing+BK15.

4.2 Analysis

Left panel from Figure 2 presents the marginalised likelihood probability distributions of the inflationary parameters, A_s , n_s , r and \mathcal{N} from the fit of the EGB dark Higgs inflation model with the PLANCK TT,TE,EE+lowE+lensing+BK15 dataset. These predictions are computed at pivot scale $k_* = 0.002 \text{ Mpc}^{-1}$ and include the uncertainty in the number of e-folds. For comparison, we also show the corresponding 65% and 95% limits from the fit of Λ CDM model with the same dataset [2]. The right panel from the same figure presents the joint confidence regions (68% and 95% CL) of n_s and r .

The mean values and the errors for all parameters are presented in Table 2.

We find that the EGB dark Higgs inflation model is strongly favoured by the PLANCK+BK15 data [2].

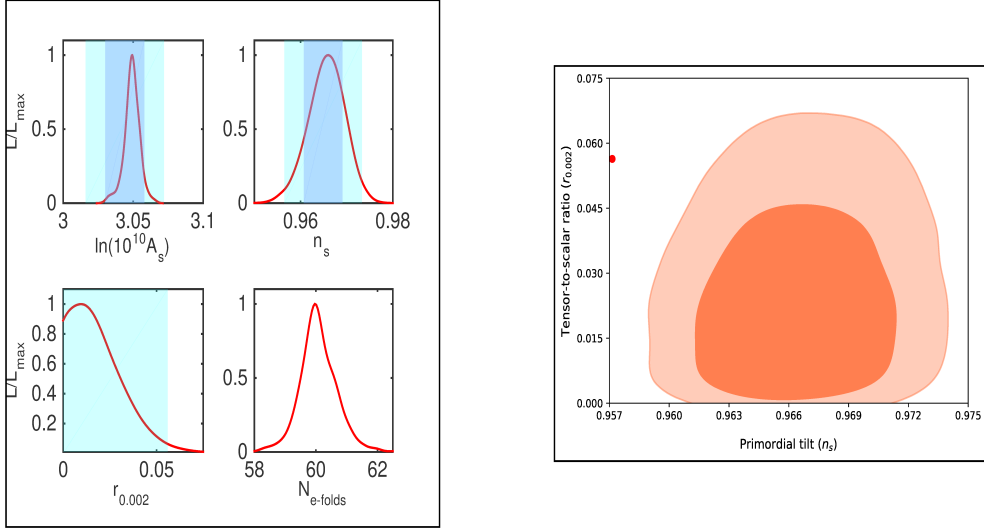


Figure 2. *Left:* Marginalised likelihood probability distributions of the main inflationary parameters from the fit of the EGB dark Higgs inflation model with the PLANCK TT,TE,EE+lowE+lensing+BK15 dataset. The distributions are obtained at $k_*=0.002 \text{ Mpc}^{-1}$ and include the uncertainty in the number of e-folds. For comparison we also show the corresponding 65% (dark blue) and 95% (light blue) limits from the fit of Λ CDM model with the same dataset [2]. *Right:* Marginalised joint 68% and 95% CL regions for n_s and r distributions presented in the left panel.

We test the consistency of the EGB dark Higgs inflation model predictions for the mean values of $\gamma\beta$, $\eta\beta$ and \mathcal{N} given in Table 2. From (3.16) we evaluate the dark Higgs field at the beginning of inflation, $\phi_I = 10.36M_{pl}$. The slow-roll parameters at ϕ_I defined in (3.14) are given by:

$$\epsilon_0 = \epsilon_1 = 0.0163, \quad k_0 = 0.0017, \quad k_1 = 0.0165, \quad \Delta_0 = 0.0249, \quad \Delta_1 = 0.0165, \quad (4.5)$$

while the tensor-to-scalar ratio (3.12) and the amplitude of the curvature perturbations (3.9) at ϕ_I are:

$$r = 0.065, \quad \mathcal{P}_R = 1.472 \times 10^{-9}. \quad (4.6)$$

The inflation potential (1.1) at ϕ_I is obtained as:

$$V^{1/4}(\phi_I) = \left(\frac{3\pi^2 \mathcal{P}_R r}{2} \right)^{1/4} M_{pl} \simeq 6.11 \times 10^{-3} M_{pl} \simeq 1.46 \times 10^{16} \text{ GeV}. \quad (4.7)$$

This constraint applied to the dark Higgs potential $V = \beta\phi_I^4/4$ leads to quartic coupling $\beta < 3.38 \times 10^{-13}$, value consistent with the inflationary observables and with the dark Higgs parameters. Under the slow-roll conditions, we get from (4.7) the Hubble parameter at ϕ_I :

$$H(\phi_I) \simeq 1.51 \times 10^{-5} M_{pl} \simeq 3.63 \times 10^{13} \text{ GeV}. \quad (4.8)$$

From (4.8) it follows that the curvature scale at ϕ_I satisfy the condition $R \simeq 12H^2 \ll M_{pl}^2$ and therefore the unitarity bound of dark Higgs inflation model with curvature couplings is not exceeded.

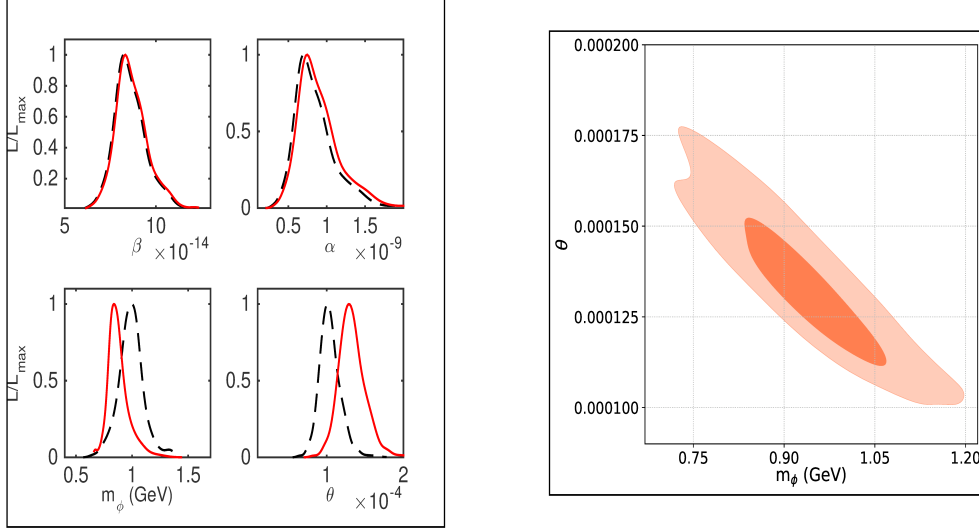


Figure 3. *Left:* Marginalised likelihood probability distributions of the dark Higgs parameters from the fit of the EGB dark Higgs inflation model with the PLANCK TT,TE,EE+lowE+lensing+BK15 dataset, obtained with (red) and without (dashed black) quantum corrections. *Right:* Marginalised joint 68% and 95% CL regions for m_ϕ and θ obtained for EGB dark Higgs inflation model.

Left panel from Figure 3 presents the likelihood probability distributions of the dark Higgs parameters β , α , m_ϕ and θ obtained from the fit of the EGB dark Higgs inflation model with the PLANCK TT,TE,EE+lowE+lensing+BK15 dataset. These predictions are computed at $k_* = 0.002 \text{ Mpc}^{-1}$ and include the quantum corrections of the coupling constants. The mean values and the errors of these parameters are given in Table 2. For comparison we plot the same distributions without quantum corrections.

The dark Higgs mass m_ϕ and mixing angle θ are derived parameters in our analysis and are obtained from (2.4). The predictions of the EGB dark Higgs inflation model for the joint confidence regions (68% and 95% CL) of m_ϕ and θ are shown in the right panel of Figure 3. We find for the dark Higgs - SM Higgs coupling, $7 \times 10^{-10} < \alpha < 3 \times 10^{-8}$. These bounds are in agreement with the estimate of the reheating temperature for a non-thermal distribution of the inflaton field [40].

The bounds on the dark Higgs mass and mixing angle are found to be:

$$0.49 \text{ GeV} < m_\phi < 1.43 \text{ GeV}, \quad (95\% \text{ CL}) \quad (4.9)$$

$$4.48 \times 10^{-5} < \theta < 1.88 \times 10^{-4}. \quad (4.10)$$

5 Dark Higgs inflaton at LHC experiments

5.1 Dark Higgs inflaton decay inside detector

The dark Higgs decay widths are suppressed by θ^2 relative to those of the SM Higgs boson if it would have the same mass as the dark Higgs. For $m_\phi < 2m_\pi$ the inflaton mostly decays in e^+e^- , $\mu^+\mu^-$ and $\tau^+\tau^-$ with decay width given by:

$$\Gamma(\phi \rightarrow \bar{l}l) = G_F \frac{m_l^2 m_\phi}{4\sqrt{2}\pi} \beta_l^3 \theta^2 \quad (l = e, \mu, \tau), \quad (5.1)$$

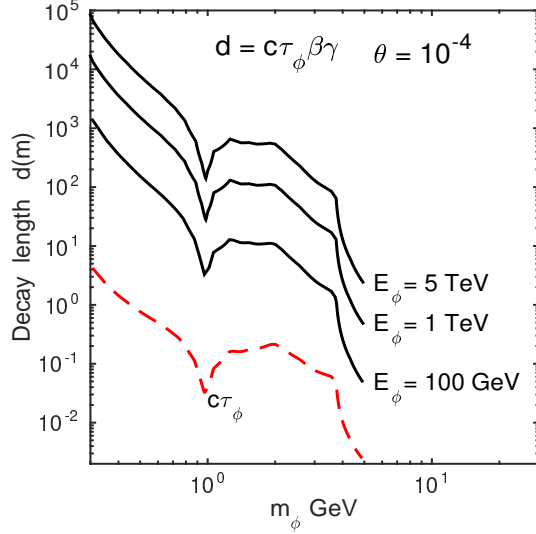


Figure 4. The evolution with m_ϕ of dark Higgs inflaton decay length, $d = c\tau_\phi\gamma\beta$, for various dark Higgs energies E_ϕ and $\theta = 10^{-4}$.

where G_F is the Fermi constant and $\beta_l = \sqrt{1 - m_l^2/m_\phi^2}$ is the lepton velocity.

For inflaton masses in the range $2m_\pi < m_\phi < 2.5$ GeV the dominant decay modes are to $\pi^+\pi^-$, k^+k^- and other hadrons.

The dark Higgs hadronic decay modes suffers from theoretical uncertainties since the chiral expansion breaks down above $2m_\pi$ while the perturbative QCD calculation are reliable for masses of few GeV [60, 61].

For the inflaton mass range (4.9) we adopt the numerical results from [61] that uses the dispersive analysis for $2m_\pi < m_\phi < 1.3$ GeV [62], the perturbative spectator model [63, 64] for $m_\phi > 2$ GeV and interpolate between these two for $1.3 \text{ GeV} < m_\phi < 2$ GeV.

Figure 4 presents the dependence on E_ϕ of the dark Higgs decay length:

$$d = c\tau_\phi\gamma\beta \quad (5.2)$$

where $\tau_\phi = 1/\Gamma(\phi \rightarrow ll, hh)$ is the dark Higgs lifetime, $\Gamma(\phi \rightarrow ll, hh)$ is the decay width scaled with θ^2 , $\gamma = E_\phi/m_\phi$ and $\beta = \sqrt{1 - 1/\gamma^2}$. The decay length scales as $d \sim E_\phi$ for large E_ϕ . For $E_\phi \sim \mathcal{O}(10^3)$ GeV the decay lengths are $d \sim \mathcal{O}(1)$ km and therefore a significant number of dark Higgs inflatons can decay within the detector volume.

To determine the number of dark Higgs inflatons that decay inside the detector volume, we must specify the size, shape, and location of the detector relative to the LHC collider interaction point (IP).

We consider two representative experiments, FASER (the ForwARd Search ExpeRiment) [36] and MAPP-1 (the MoEDAL Apparatus for Penetrating Particles) ([65]).

FASER detectors have cylindrical shape and are centred on the LHC beam collision axis. The detectors have the radius R and the depth $\Delta = L_{max} - L_{min}$, where L_{max} and L_{min} are the distances from the IP to the far and near edge of detectors along the beam axis. The location of FASER detectors is:

$$\text{FASER far location : } L_{max} = 400 \text{ m}, \Delta = 10 \text{ m}, R = 1 \text{ m}, \quad (5.3)$$

$$\text{FASER near location : } L_{max} = 150 \text{ m}, \Delta = 5 \text{ m}, R = 4 \text{ cm}. \quad (5.4)$$

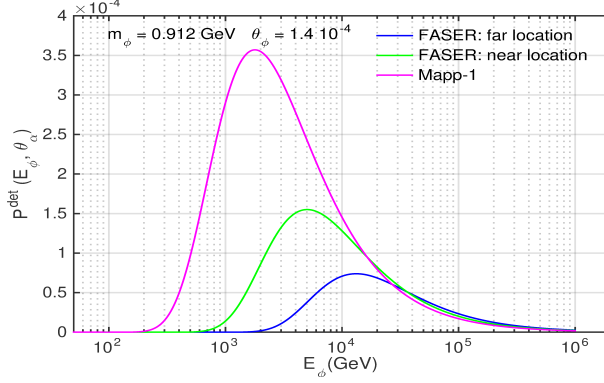


Figure 5. The dependence on the dark Higgs energy E_ϕ of the normalised detection probability corresponding to different experimental configurations obtained for cosmological best fit solution for m_ϕ and θ .

MAPP detector is a parallelepiped at approximately 5^0 from the beam collision axis with the following location:

$$\text{MAPP} - 1 : \quad L_{max} = 55 \text{ m}, \Delta = 3 \text{ m}, H = 1 \text{ m}, \quad (5.5)$$

where H is the is the parallelepiped height.

The probability of the dark Higgs boson to decay inside the detector volume is given by:

$$\mathcal{P}^{det}(E_\phi, \theta_\alpha) = \left(e^{-L_{min}/d} - e^{-L_{max}/d} \right) \Theta(R, \tan(\theta_\alpha)L_{max}) \quad (5.6)$$

where E_ϕ is the dark Higgs energy, d is its decay length, θ_α is the angular acceptance of the detector, $\tan(\theta_\alpha) = R/L_{max}$, and Θ is the Heaviside step function. For MAPP-1 we take $R = H\pi^{-1/2}$ in (5.6) to conserve the effective acceptance area.

In Figure 5 we present the dependence on E_ϕ of the normalised detection probability corresponding to the different experimental configurations obtained for cosmological best fit solution for m_ϕ and θ . The figure shows that the experimental configurations are sensitive to complementar ranges of the dark Higgs energy.

5.2 Dark Higgs inflaton production at LHC

The dark Higgs bosons are mainly produced through K and B meson decays. As $m_\phi > m_K$ ($m_K = 0.494$ GeV) for the inflaton mass range (4.9), in the following we consider the dark Higgs production only through the B-meson decay. The B-meson branching fraction is given by [36]:

$$Br(B \rightarrow X_s \phi) = 5.7 \left(1 - \frac{m_\phi^2}{m_B^2} \right)^2 \theta^2, \quad (5.7)$$

where X_s denotes any strange hadronic state and m_B is the B-meson mass ($m_B = 5.28$ GeV).

The dark Higgs production cross section at LHC energies can be estimated as [45]:

$$\frac{\sigma_\phi}{\sigma_{inel}} = M_{pp} Br(B \rightarrow X_s \phi), \quad (5.8)$$

where M_{pp} is the proton multiplicity and σ_{inel} is the pp inelastic cross section.

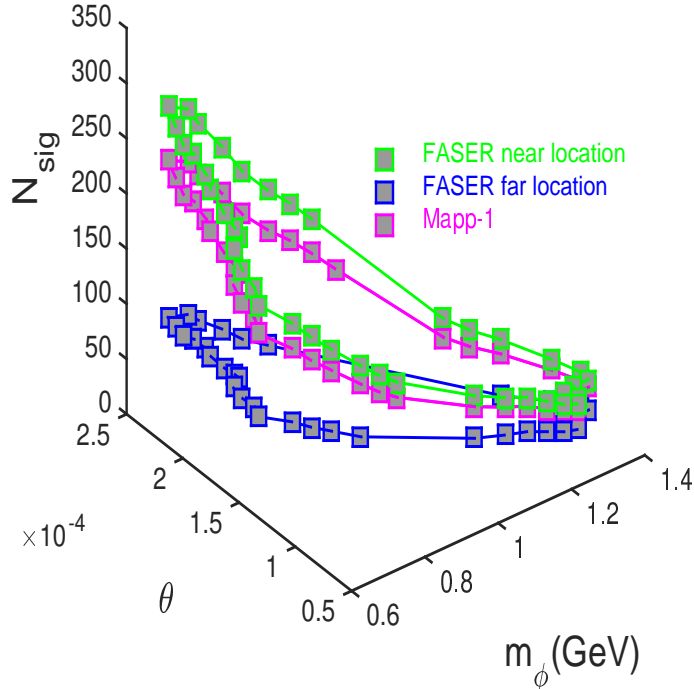


Figure 6. LHC experiments reach for dark Higgs inflaton in the cosmological confidence region (4.9) for an integrated luminosity of $3ab^{-1}$ at 13 TeV LHC assuming 100% detection efficiency.

5.3 LHC experiments reach for dark Higgs inflaton

The total number of dark Higgs bosons that decay inside detector are then given by:

$$N_{sig}(m_\phi, \theta) = N_{inel} \frac{\sigma_\phi}{\sigma_{inel}} Br(\phi \rightarrow KK) Br(\phi \rightarrow \pi\pi) \int \mathcal{P}^{det}(E_\phi, \theta_\alpha) d\theta_\alpha dE_\phi, \quad (5.9)$$

where N_{inel} is the total number of inelastic pp scattering events.

Throughout we assume an integrated luminosity of $3 ab^{-1}$ at the 13 TeV LHC, implying $N_{inel} \simeq 1.1 \times 10^{16}$. We also take $\sigma_{inel}(13 \text{ TeV}) \simeq 75 \text{ mb}$ and $M_{pp}(13 \text{ TeV}) \simeq 66$ [31].

Figure 6 shows the predicted number of dark Higgs inflaton decays in the cosmological confidence region (4.9) obtained for the experimental configurations discussed for an integrated luminosity of $3ab^{-1}$ at 13 TeV LHC assuming 100% detection efficiency.

In our computation we take the dark Higgs energy in the range $100 \text{ GeV} < E_\phi < 10^6 \text{ GeV}$, imposed by the requirement that the dark Higgs inflaton propagate to the detector locations, as shown in Figure 5.

For comparison, in Figure 7 we present the FASER reach [36] and the MAPP-1 reach [65] for the dark Higgs boson for an integrated luminosity of $3ab^{-1}$ at 13 TeV LHC. The cosmological dark Higgs inflaton confidence region (4.9) is also shown.

6 Conclusion

In this paper we analyse the dark Higgs inflation model with curvature corrections given by the kinetic term non-minimally coupled to the Einstein tensor and the coupling to the Gauss-Bonnet (GB) 4-dimensional invariant (EGB dark Higgs inflation) and explore the possibility

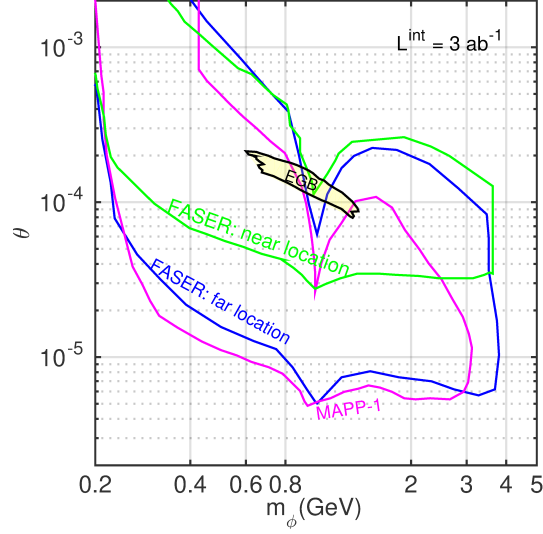


Figure 7. FASER far location, FASER near location and MAPP-1 reach for dark Higgs boson for an integrated luminosity of 3ab^{-1} at 13 TeV LHC. The cosmological dark Higgs inflaton confidence region (4.9) is also shown.

Table 2. The mean values and the absolute errors of the main parameters obtained from the fit of the EGB dark Higgs inflation model with PLANCK TT,TE,EE+lowE+lensing+BK15 dataset. The errors are quoted at 68% CL. The upper limits are quoted at 95% CL. The first group of parameters are the base cosmological parameters sampled in the Monte-Carlo Markov Chains analysis with uniform priors. The others are derived parameters.

Parameter	
$\Omega_b h^2$	0.0223 ± 0.0002
$\Omega_c h^2$	0.1194 ± 0.0011
θ_s	1.0410 ± 0.0004
τ	0.050 ± 0.009
$\ln(10^{10} A_s)$	3.050 ± 0.008
n_s	0.967 ± 0.0044
$r_{0.002}$	< 0.059
\mathcal{N}	59.4 ± 1.210
$10^{13} \times \beta$	0.892 ± 0.051
$10^9 \times \alpha$	1.021 ± 0.219
$\gamma\beta$	0.218 ± 0.015
$\eta\beta$	1.129 ± 0.067
$H_0(\text{km s}^{-1}\text{Mpc}^{-1})$	67.729 ± 0.641
m_ϕ (GeV)	0.919 ± 0.211
$10^4 \times \theta$	1.492 ± 0.045

to test its predictions by particle physics experiments at LHC.

The dynamics of the slow-roll inflation with curvature corrections has been proposed in context of the SM Higgs inflation in Refs [14, 15].

We show that the EGB dark Higgs inflation model is strongly favoured by PLANCK+BK15 data [2]. The cosmological predictions of this model for dark Higgs inflaton mass m_ϕ and mixing angle θ , including the RG quantum corrections of dark Higgs coupling constants and the uncertainty in estimation of the reheating temperature, are found to be:

$$\begin{aligned} 0.49 \text{ GeV} < m_\phi < 1.34 \text{ GeV}, & \quad (95\% \text{ CL}) \\ 4.48 \times 10^{-5} < \theta < 1.88 \times 10^{-4}. \end{aligned}$$

The consistency test of the EGB dark Higgs inflation model predictions leads to a lower bound of dark Higgs inflaton quartic coupling $\beta < 3.38 \times 10^{-13}$, value consistent with the inflationary observables and with the dark Higgs parameters.

We find the dark Higgs inflaton - SM Higgs boson coupling constant $\alpha > 7 \times 10^{-10}$, in agreement with the estimate of the reheating temperature for a non-thermal distribution of the inflaton field [40].

We evaluate the FASER and MAPP-1 experiments reach for dark Higgs inflaton parameters m_ϕ and θ in the 95% CL cosmological confidence region, for an integrated luminosity of 3ab^{-1} at 13 TeV LHC assuming 100% detection efficiency.

We conclude that the dark Higgs inflation model with curvature corrections is a compelling inflation scenario based on particle physics theory favoured by the present cosmological measurements that leaves imprints in the dark Higgs boson searches at LHC.

Acknowledgments

The author would like to thank to Vlad Popa for helpful discussions and acknowledge the use of the GRID system computing facility at the Institute of Space Science. This work was partially supported by ESA/PRODEX Contract 4000124902.

References

- [1] Planck Collaboration; N. Aghanim, et al., *Planck 2018 results VI. Cosmological parameters*, *A & A* **641** (2020) A10 [arXiv:1807.06209].
- [2] Planck Collaboration; N. Aghanim et al., *Planck 2018 results. X. Constraints on inflation*, *A & A* **641** (2020) A6 [arXiv:1807.06211].
- [3] P. A. R. Ade et al., *BICEP2 / Keck Array X: Constraints on Primordial Gravitational Waves using Planck, WMAP, and New BICEP2/Keck Observations through the 2015 Season*, *Phys. Rev. Lett.* **121** (2018) 221301 [arXiv:1810.05216].
- [4] ATLAS Collaboration Collaboration, G. Aad et al., *Observation of a new particle in the search for the Standard Model Higgs boson with the ATLAS detector at the LHC*, *Phys.Lett.* **B716** (2012) 1 [arXiv:1207.7214].
- [5] CMS Collaboration Collaboration, S. Chatrchyan et al., *Observation of a new boson at a mass of 125 GeV with the CMS experiment at the LHC*, *Phys.Lett.* **B 716** (2012) 30 [arXiv:1207.7235].
- [6] J. Beacham, et al., *Physics Beyond Colliders at CERN Beyond the Standard Model Working Group Report*, *J. Phys. G* **47** (2020) 1, 010501 [arXiv:1901.09966]
- [7] F. L. Bezrukov and M. Shaposhnikov, *The Standard Model Higgs boson as the inflaton*, *Phys. Lett.* **B 659** (2008) 703 [arXiv:0710.3755].

- [8] T. Futamase and K.-I. Maeda, *Chaotic Inflationary Scenario in Models Having Nonminimal Coupling With Curvature*, *Phys. Rev. D* **39** (1989) 399.
- [9] R. Fakir and W. G. Unruh, *Improvement on cosmological chaotic inflation through nonminimal coupling*, *Phys. Rev. D* **41** (1990) 1783.
- [10] C. Germani and A. Kehagias, *New Model of inflation with Nonminimal Derivative Coupling of Standard Model Higgs Boson to Gravity*, *Phys. Rev. Lett.* **105** (2010) 011302.
- [11] L. N. Granda, *Inflation driven by scalar field with non-minimal kinetic coupling with Higgs and quadratic potentials*, *JCAP* **04** (2011) 016 [arXiv:1104.2253]
- [12] L. N. Granda, D. F. Jimenez, W. Cardona, *Higgs inflation with non-minimal derivative coupling to gravity* *Astropart. Phys.* **121** (2020) 102459 [arXiv:1911.02901]
- [13] S. Tsujikawa, *Observational tests of inflation with a field derivative coupling to gravity*, *Phys. Rev. D* **85** (2012) 083518 [arXiv:1201.5926].
- [14] L. N. Granda and D. F. Jimenez, *Higgs Inflation with linear and quadratic curvature corrections* [arXiv:1910.11289].
- [15] L. N. Granda and D. F. Jimenez, *Slow-Roll Inflation in Scalar-Tensor Models*, *JCAP* **09** (2019) 007 [1905.08349].
- [16] K. Kamada, T. Kobayashi, M. Yamaguchi, J. Yokoyama, *Higgs G-inflation* *Phys. Rev. D* **83** (2011) 083515.
- [17] J. Ohashi and S. Tsujikawa, *Potential-driven Galileon inflation*, *JCAP* **1210** (2012) 035 [arXiv:1207.4879].
- [18] T. Kobayashi, M. Yamaguchi, J. Yokoyama, *Inflation Driven by the Galileon Field*, *Phys. Rev. Lett.* **105** (2010) 231302.
- [19] T. Kobayashi, M. Yamaguchi, J. Yokoyama, *Generalized G-inflation: Inflation with the most general second-order field equations*, *Prog. Theor. Phys.* **126** (2011) 511 [arXiv:1105.5723].
- [20] C. P. Burgess, H. M. Lee, M. Trott, *Power-counting and the Validity of the Classical Approximation During Inflation*, *JHEP* **09** (2009) 103 [arXiv:0902.4465].
- [21] F. Bezrukov, A. Magnin, M. Shaposhnikov, S. Sibiryakov, *Higgs inflation: consistency and generalisations*, *JHEP* **011** (2011) 016 [arXiv:1008.5157].
- [22] C. P. Burgess, S. P. Patil, T. Michael, *On the predictiveness of single-field inflationary models*, *JHEP* **06** (2014) 10 [arXiv:1402.1476]
- [23] A. D. Linde, *Chaotic inflation*, *Phys. Lett. B* **129** (1983) 177.
- [24] J. Bramante, J. Cook, A. Delgado, A. Martin *Low scale inflation at high energy colliders and meson factories*, *Phys. Rev. D* **94** (2016) 115012
- [25] G. German, *Quartic hilltop inflation revisited*, *JCAP* **02** (2021) 034 [arXiv:2011.12804].
- [26] M. Atkins, X. Calmet, *Remarks on Higgs inflation*, *Phys. Lett. B* **697** (2011) 37 [arXiv:1011.4179].
- [27] F. Bezrukov, J. Rubio and M. Shaposhnikov, *Living beyond the edge: Higgs inflation and vacuum metastability*, *Phys. Rev. D* **92** (2015) 083512 [arXiv:1412.3811].
- [28] D. Buttazzo, G. Degrassi, P. P. Giardino, G. F. Giudice, F. Sala, A. Salvio and A. Strumia, *Investigating the near-criticality of the Higgs boson*, *JHEP* **12** (2013) 089 [arXiv:1307.3536].
- [29] G. Degrassi, S. Di Vita, J. Elias-Miro, J. R. Espinosa, G. F. Giudice, G. Isidori, A. Strumia, *Higgs mass and vacuum stability in the Standard Model at NNLO*, *JHEP* **08** (2012) 098 [arXiv:1205.6497].
- [30] K. Allison, *Higgs xi-inflation for the 125-126 GeV Higgs: a two-loop analysis*, *JHEP* **02**

- (2014) 040 [arXiv:1306.6931].
- [31] P.A. Zyla et al., *Particle Data Group, Prog. Theor. Exp. Phys.* **2020** (2020) 083C01.
- [32] O. Lebedev, *On Stability of the Electroweak Vacuum and the Higgs Portal*, *Eur. Phys. J.* **72** (2012) 2058 [arXiv:1203.0156].
- [33] J. Elias-Miro, J. R. Espinosa, G. F. Giudice, H. M. Lee, A. Strumia, *Stabilization of the Electroweak Vacuum by a Scalar Threshold Effect*, *JHEP* **06** (2012) 031 [arXiv:1203.0237].
- [34] G. Ballesteros and C. Tamarit, *Higgs portal valleys, stability and inflation*, *JHEP* **09** (2015) 210 [arXiv:1505.07476].
- [35] J. R. Ellis, M. K. Gaillard, and D. V. Nanopoulos, *A phenomenological profile of the Higgs boson*, *Nucl. Phys.* **B 106** (1976) 292.
- [36] J. L. Feng, I. Galon, F. Kling, S. Trojanowski, *Dark Higgs bosons at the ForwArd Search ExpeRiment*, *Phys. Rev.* **D 97** (2018) 055034 [arXiv:1710.09387].
- [37] M. Shaposhnikov and I. Tkachev, *The ν MSM inflation and dark matter*, *Phys. Lett.* **B 639** (2006) 414 [arXiv: 0604236].
- [38] T. Asaka, S. Blanchet, and M. Shaposhnikov, *The MSM, dark matter and neutrino masses*, *Phys. Lett.* **B 631** (2005) 151 [arXiv:0503065].
- [39] T. Asaka and M. Shaposhnikov, *The MSM dark matter and baryon asymmetry of the universe*, *Phys. Lett.* **B 620** (2005) 17 [arXiv:0505013].
- [40] A. Anisimov, Y. Bartocci, F. L. Bezrukov, *Inflaton mass in the ν MSM inflation*, *Phys. Lett.* **B 671** (2009) 211 [arXiv:0809.1097].
- [41] R. N. Lerner and J. McDonald, *Distinguishing Higgs inflation and its variants*, *Phys. Rev.* **D 83** (2011) 123522 [arXiv:1104.2468].
- [42] T. Tenkanen, K. Tuominen and V. Vaskonen, *A Strong Electroweak Phase Transition from the Inflaton Field*, *JCAP* **09** (2016) 037 [arXiv:1606.06063].
- [43] A. Aravind, M. Xiao and J. H. Yu, *Higgs Portal to Inflation and Fermionic Dark Matter* *Phys. Rev.* **D 93** (2016) 123513 [arXiv:1512.09126].
- [44] J. Kim, P. Ko, W. Park, *Higgs-portal assisted Higgs inflation with a sizeable tensor-to-scalar ratio*, *JCAP* **02** (2017) 003 [arXiv:1405.1635].
- [45] F. Bezrukov and D. Gorbunov, *Light inflaton Hunter’s Guide*, *JHEP* **05** (2010) 010 [arXiv:0912.0390].
- [46] F. Bezrukov, D. Gorbunov, *Light inflaton after LHC8 and WMAP9 results*, *JHEP* **07** (2013) 140 [arXiv:1303.4395].
- [47] P. X. Jiang, J. W. Hu and Z. K. Guo, *Inflation coupled to a Gauss-Bonnet term*, *Phys. Rev.* **D 88** (2013) 123508 [arXiv:1310.5579].
- [48] P. Kanti, R. Gannouji and N. Dadhich, *Gauss-Bonnet Inflation*, *Phys. Rev.* **D 92** (2015) 041302 [arXiv:1503.01579].
- [49] S.D. Odintsov, V.K. Oikonomou, *Viable Inflation in Scalar-Gauss-Bonnet Gravity and Reconstruction from Observational Indices*, *Phys. Rev.* **D 98** (2018) 044039 [arXiv:1808.05045].
- [50] D. H. Lyth and A.A. Riotto, *Particle physics models of inflation and the cosmological density perturbation*, *Phys. Rep.* **314** (1999) 1 [arXiv: 9807278].
- [51] R. Micha and I.I. Tkachev, *Relativistic Turbulence: A Long Way from Preheating to Equilibrium*, *Phys. Rev. Lett.* **90**(2003) 121301 [hep-ph/0210202].
- [52] R. Micha and I.I. Tkachev, *Turbulent Thermalization*, *Phys.Rev.* **D 70** (2004) 043538,

[hep-ph/0403101].

- [53] A. Aravind, M. Xiao and J. H. Yu, *Higgs Portal to Inflation and Fermionic Dark Matter*, *Phys. Rev. D* **93** (2016) 123513 [arXiv:1512.09126].
- [54] W. H. Kinney and A. Riotto, *Theoretical uncertainties in inflationary predictions*, *JCAP* **03** (2006) 011 [arXiv:0511127].
- [55] A. O. Barvinsky, A. Yu. Kamenshchik, C. Kiefer, A. A. Starobinsky, C. F. Steinwachs, *Higgs boson, renormalization group, and naturalness in cosmology*, *JCAP* **12** (2009) 003 [arXiv:0910.1041].
- [56] A. Lewis, A. Challinor, A. Lasenby, *Efficient computation of CMB anisotropies in closed FRW models*, *ApJ* **538** (2000) 473.
- [57] A. Lewis, S. Bridle, *Cosmological parameters from CMB and other data: A Monte Carlo approach*, *Phys. Rev. D* **66** (2002) 103511.
- [58] Planck Collaboration; N. Aghanim, et al., *Planck 2018 results. V. Power spectra and likelihoods*, *A & A* **641** (2020) A5 [arXiv:1907.12875].
- [59] Planck Collaboration; N. Aghanim, et al., *Planck 2018 results. VIII. Gravitational lensing*, *A & A* **641** (2020) A8 [arXiv:1807.06210].
- [60] J. D. Clarke, R. Foot, and R. R. Volkas, *Phenomenology of a very light scalar ($100 \text{ MeV} < m_h < 10 \text{ GeV}$) mixing with the SM Higgs*, *JHEP* **02** (2014) 123 [arXiv:1310.8042].
- [61] M. W. Winkler, *Decay and Detection of a Light Scalar Boson Mixing with the Higgs*, *Phys. Rev. D* **99** 015018 [arXiv:1809.01876].
- [62] B. Grinstein, L. J. Hall, and L. Randall, *Decay and Detection of a Light Scalar Boson Mixing with the Higgs*, *Phys. Lett. B* **211** (1988) 363.
- [63] J. F. Gunion, H. E. Haber, G. L. Kane, and S. Dawson, *The Higgs Hunter's Guide*, *Front. Phys.* **80** (2000) 1.
- [64] D. McKeen, *Constraining Light Bosons with Radiative $\gamma(1S)$ Decays*, *Phys. Rev. D* **79** (2009) 015007 [0809.4787].
- [65] J. L. Pinfold, *The MoEDAL experiment: a new light on the high-energy frontier*, *Phil. Trans. R. Soc. A* **377** 20190382.